

# **Nuclear Reaction Mechanisms of Neutron Induced Fission of** <sup>237</sup>**Np Nucleus**

Cristiana Oprea<sup>1,2\*</sup>, Mohammad Ayaz Ahmad<sup>3</sup>, Alexandru Ioan Oprea<sup>1</sup>, Jalal H. Baker<sup>3</sup>, Naima Amrani<sup>4</sup>

- <sup>1</sup> Joint Institute for Nuclear Research (JINR), Frank Laboratory of Neutron Physics (FLNP), Joliot-Curie 6, Dubna 141980, Moscow Region, Russian Federation
- <sup>2</sup> Romanian National Agency for Scientific Research, 21-25 Mendeleev, 010362, Sector 1. Bucharest
- <sup>3</sup> Physics Department, Faculty of Science, P.O.Box 741, University of Tabuk, 71491, Saudi Arabia
- <sup>4</sup> Ferhat Abbas University of Setif, Laboratory for Dosage and Analysis of Characteristic in height resolution (DAC), Department of Physics, Sétif, Algeria

#### ARTICLE INFO

#### **Keywords:**

Neutron Fission, Cross-Sections, Fission Yields, Nuclear Reaction Mechanisms, Isotopes

#### **ABSTRACT**

At FLNP JINR Dubna new prospects for developing new neutron facilities have already been started, that will replace the IBR-2 neutron pulsed research reactor which shut down in the year 2032. Several agreed projects use the fission processes induced by neutrons on neptunium-based fuels. An investigation of the neutron fission process on the <sup>237</sup>Np nucleus was conducted in the present research. Several parameters were analyzed during neutron-induced fission of <sup>237</sup>Np including the neutron cross-section, mass distributions, prompt neutron emission, isotope production, and neutron spectra. Evaluations of the above observables were conducted using TALYS – 9.1 Software, with incident neutron energies ranging from 0.4 to 25 MeV. The exact value of cross-section was obtained as 5 - 5.5 MeV in the present work, whereas from literature, it was found up to 10 MeV. Neutron spectra were analyzed and separated contributions from different nuclear reaction mechanisms were obtained. Our investigations have revealed some important yields and isotope production cross-sections that were in good agreement with literature data.

## 1. Introduction

Throughout modern science, neutrons have been successfully used in fundamental researches to investigate nuclear interactions, symmetry issues, and the structure of atomic nuclei. Neutrons are used in applied sciences in fields such as condensed matter physics, molecular biology, structural chemistry, materials science, nondestructive metallography, and industrial processes. Modern science research advances necessitate the development of more intense neutron sources. In neutron scattering experiments, an increase in the neutron flux intensity allows for more efficient neutron research. This is because the time of experiments can be reduced, the accuracy of measurements improves and a variety of new opportunities open up

## Cite this article as:

Oprea, C., Ahmad, M. A., Oprea, A. I., Baker, J. H., & Amrani. N. (2021). Nuclear Reaction Mechanisms of Neutron Induced Fission of <sup>237</sup>Np Nucleus. *European Journal of Engineering Science and Technology*, 4(4): 15-24. https://doi.org/10.33422/ejest.v4i4.600

© The Author(s). 2021 **Open Access**. This article is distributed under the terms of the <u>Creative Commons Attribution 4.0 International License</u>, <u>which permits</u> unrestricted use, distribution, and redistribution in any medium, provided that the original author(s) and source are credited.



<sup>\*</sup>Corresponding author E-mail address: coprea2007@yahoo.co.uk

with regard to studying small, complex objects (Aksenov et. al., 2017, A), (Aksenov, 2017, B).

## 1.1. Neptunium-237

A silver-gray metal, Neptunium is a good conductor of electricity and heat. Its melting point is 637 °C and its boiling point is 4175 °C (Thomassin et al., 2001). The element exists in five oxidation states, from III to VII and belongs to the actinide family. Neptunium is the first element in the transuranic group; its twenty-two isotopes range from <sup>225</sup>Np to <sup>242</sup>Np. All of them are radioactive, and most of them have very short half-lives.

Among of all Neptunium isotopes,  $^{237}Np$  is the most important one; it is a radioactive artificial nucleus with an atomic mass A=237 and a proton number Z=93. This is the radioactive element with the longest half-life of about  $2.144x10^6$  years, and mass activity of about  $2.6x10^7$  Bq.g<sup>-1</sup>.

Upon  $\alpha$  decay, <sup>237</sup>Np forms <sup>233</sup>Pa, which is itself a  $\beta$  emitter with half-live of 27 days. Significant amounts of <sup>237</sup>Np are produced in nuclear reactors by burning <sup>238</sup>U in accordance with the reactions (Audi et al., 2003, A), (Audi et al., 2003, B):

$$^{238}U(n,2n)^{237}U \xrightarrow{\beta} ^{237}Np \tag{1}$$

$$^{235}U(n,\gamma)^{236}U(n,\gamma)^{237}U \xrightarrow{\beta} ^{237}Np \tag{2}$$

Its contribution consists in long-term high-level waste (HLW) radiotoxicity of nuclear spent fuel.

## 1.2. Neutron-Induced Fission on Neptunium-237

In the spent fuel from nuclear power plants, <sup>237</sup>Np is present in a noteworthy amount. As a result of the neutron fission process with long-lived actinides, these can be incinerated and used as nuclear fuel in nuclear reactors. Compared to conventional <sup>235</sup>U and <sup>239</sup>Pu fuels, <sup>237</sup>Np has a fission cross-section of a threshold type. It is estimated that the effective fission threshold for <sup>237</sup>Np is around 0.4 MeV, which is 0.2 MeV lower than that of <sup>238</sup>U. (Shabalin et al., 2017, A), (Shabalin et al., 2017, B) emphasize the importance of this property in evaluating the critical mass. Fast neutron-induced fission of <sup>237</sup>Np produces delayed neutrons with a time of life three orders of magnitude lower than that of <sup>238</sup>U and <sup>239</sup>Pu. In the light of the properties of <sup>237</sup>Np mentioned above, this long-lived actinide isotope may prove useful as a future fuel for research nuclear reactors (Shabalin et al., 1966), (Aksenov et al, 2017, A), (Aksenov et al, 2017, C).

The data on <sup>237</sup>Np (n, f) can be found from a variety of sources. It is possible to obtain experimental data from EXFOR database and evaluated data from nuclear data libraries (ENDF/B-VII.1, JENDL-4.0, JEFF3.2, CENDL 3.1, ROSFOND-2010), which are useful especially when experimental data are lacking.

The processes induced by fast neutrons with energy ranging from 0.4 MeV up to 25 MeV were studied in the present investigation to evaluate nuclear reaction mechanisms and fission variables. These variables include cross-sections, mass distributions, prompt neutron emission, isotope productions, as well as neutron spectra.

## 2. Computer Codes and Nuclear Reaction Mechanisms

We have evaluated variables of fission under various reaction mechanisms using Talys and programs designed by the authors.

## 2.1. Talys Code

TALYS is software for the analysis and prediction of nuclear reactions involving neutrons, photons, protons, deuterons, tritons, <sup>3</sup>He- and alpha-particles within the energy range of *I* keV to 200 MeV and for target nuclides of mass 5 u.a. and heavier. In order to accomplish this, various nuclear reaction models have been integrated into one code system. It allows a detailed evaluation of nuclear reactions from the unresolved resonance range until intermediate energies are reached (Koning et al., 2007), (Koning et al., 2008).

TALYS is a nuclear physics tool that allows the modeling of nuclear reactions and the generation of nuclear data when measurements are not available (Koning & Rochman, 2012).

Calculations using the TALYS code can produce the following results: Total cross-sections, Elastic and Non-elastic cross-sections, Elastic scattering angular distributions, Inelastic scattering angular distributions, and Cross-sections to discrete states, Cross sections of exclusive channels, i.e.  $(n,\gamma)$ , (n,2n), (n,np),..., with their energy spectra and double differential spectra, Gamma ray production for discrete and continuum states, Production cross sections of isomeric states, Fission cross sections, fission fragments and product yields, Production cross sections of residual nuclei, and Total particle emission cross sections, i.e., (n,xn), (n,xp),..., with their energy spectra and double differential spectra (Koning & Rochman, 2011).

## 2.2. Nuclear Reaction Mechanisms. Elements of Theory

By using the Hauser-Feshbach formalism, fission induced by fast neutrons can be explained by compound processes. Fission cross-section can then be modeled as follows (Hauser & Feshbach, 1952), (Koning et al., 2007):

$$\sigma_{nf}(E_n) = g\pi \lambda_n^2 T_n T_f \left[ \sum_c T_c \right]^{-1} \tag{1}$$

$$T_f^{J,\Pi}(E_x) = \sum_i T_f(E_x, \varepsilon_i) f(i, j, \Pi) + \int_{E_{th}}^{E_x} \rho(\varepsilon, j, \Pi) T_f(E_x, \varepsilon) d\varepsilon$$
 (2)

where T are the transmission coefficients; g is the statistical factor;  $\lambda_n$  is the reduced neutron wave number; c are the channels;  $E_x, E_{thr}, \varepsilon$  are the excitation, threshold, and current energies, respectively;  $J, \Pi$  are the spin and parity of the compound nucleus;  $\rho$  represents the nuclear states density.

Transmission coefficients, *T*, from relationship (2), are the probabilities of particles passing a potential barrier and can be computed for discrete and continuum states, respectively. In relation (2), the sum represents discrete states and the integral represents continuum ones (Koning et al, 2007). Levels density is derived from statistical formalisms of nuclear reactions, mainly from the Fermi gas model and combinatorial approaches (Koning et al., 2008). In the fission process transmission coefficients are calculated by using the Hill – Wheeler expressions (Koning et al, 2007).

Further fission variables, such as mass and charge distributions of fission fragments, prompt neutron distributions, and isotope yields fission product can be calculated by Brosa's model (Brosa et al., 1990). In the frame of Brosa approach, it is supposed that the fission

process is a succession of nonstable nuclear states (instant Rayleigh type of instability) where the break of the neck has an instant character. Scission occurs when the neck is flat and the location of scission is random, therefore giving the possibility of multichannel fission.

Fission barrier parameters were taken from experimental data (Koning et al., 2007) and calculated by authors in accordance with (Mamdouh et al., 2001) where sets of double–humped parameters are defined for a large number of isotopes obtained from Extended Tomas – Fermi and Strutinski integral calculations (Strutinsky, 1968).

Mass distribution (relative yields) is calculated applying the following relation (Koning et al., 2007):

$$Y(A_{FF}; Z_{FS}, A_{FS}, E_x) = \sum_{FM} W_{FM} (Z_{FS}, A_{FS}, E_x) Y_{FM} (A_{FF}; Z_{FS}, A_{FS}, E_x)$$
(3)

where  $A_{FF}$  is the fragment mass coming from a fissionable system (nucleus) with mass  $A_{FS}$  and charge  $Z_{FS}$ ;  $W_{FM}$  is the weight of a fission mode of a nucleus with mass  $A_{FS}$  and charge  $Z_{FS}$ ;  $Y_{FM}$  ( $A_{FF}$ ;  $Z_{FS}$ ,  $A_{FS}$ ,  $E_x$ ) are the relative yields of a fission mode;  $E_x$  is the excitation energy.

The production XS of the fission fragment with given mass ( $A_{FF}$ ) and charge ( $Z_{FF}$ ) is (Koning et al, 2007):

$$\sigma_{prod}\left(Z_{FF}, A_{FF}\right) = \sum_{Z_{FS}, A_{FS}, E_{x}} \sigma_{F}\left(Z_{FS}, A_{FS}, E_{x}\right) Y\left(A_{FF}; Z_{FS}, A_{FS}, E_{x}\right) Y\left(Z_{FF}; A_{FF}, Z_{FS}, A_{FS}, E_{x}\right) (4)$$

where  $Y(Z_{FF}; A_{FF}, Z_{FS}, A_{FS}, E_x)$  represent the relative yields with charge  $Z_{FF}$  and mass  $A_{FF}$  coming from the fissionable nucleus with charge  $Z_{FS}$  and mass  $A_{FS}$ .

As part of the analysis, neutron spectra were evaluated taking into account neutron evaporation from fission fragments and neutrons obtained through other possible channels. Neutron evaporation of excited fragments of fission is enabled by compound processes. Also, alongside fission, in the interaction of neutrons with fissionable nuclei, there are open elastic, inelastic, capture, and other channels, which involve the emission of light charged particles or clusters. In this case, neutrons within the spectrum are produced not only by compound mechanisms characteristic to fission and evaporation but also by direct and pre-equilibrium mechanisms from other open channels (Koning et al., 2007).

#### 3. Results and Discussions

A cross section (XS) of the neutron induced fission process starting from 0.4 MeV to 25 MeV on the nucleus  $^{237}Np$  is presented in Figure 1.

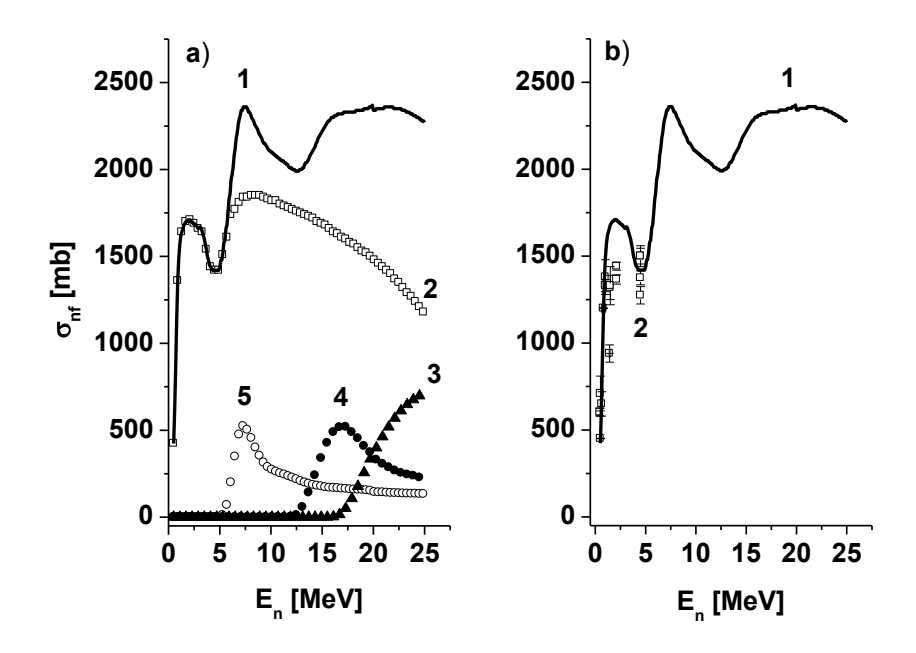


Figure. 1. <sup>237</sup>Np total fission XS. a) A contribution to the XS by fissionable nuclei derived from <sup>237</sup>Np.1-Talys; 2– $^{238}$ Np; 3– $^{237}$ Np; 4- $^{236}$ Np; 5– $^{235}$ Np b) 1–Talys; 2–Experimental Data.

In the fission process, other fissionable nuclei can be created. The shape and magnitude of total XS are affected by these isotopes (Figure 1.a). The main contribution to total XS is from the compound nucleus <sup>238</sup>Np. The XS of other Np isotopes must also be considered in the XS total after 7-8 MeV fission (curves 2, 3, and 4 from Fig. 1.a). There is no difference between curve 1 from Figure 1.a and curve 1 from Figure 1.b. As a result of the neutron interaction with  $^{237}Np$ , other fissionable isotopes of U and Pa are also formed, but their XS can be ignored. In nuclear reactor technology, the total XS of different isotopes is important. The theoretical evaluations and experimental data from various literature sources (Diakaki et al., 2016), (Jiacoletti et al., 1972), included in Figure 1.b, show a good agreement. It is noteworthy that experimental data are available only up to 10 MeV. In this report, fission XS up to 5 MeV has been described very well. A few experimental XS data for higher energies, between 14 and 16 MeV, can be found in the references (Diakaki et al., 2016), (Jiacoletti et al., 1972), (Ruskov et al., 2018). Important fission observables, such as fission fragment mass distribution and prompt neutron multiplicities, are shown in Figure 3. Pre- and post-neutron emissions of excited fission fragments are also represented for both observables. As a result of analyzing nuclear reaction mechanisms, neutron evaporation, temperature dependence, and density levels in the Brosa model, average prompt neutron multiplicity and mass distribution have been evaluated (Brosa et al., 1990). With the increase of incident neutron energy, mass distributions and average prompt neutron multiplicities become wider on fragment mass. Based on theoretical predictions, the probability of symmetrical fission and prompt neutron emission increases with neutron energy (see Figures 2.a - 2.b and 3.a - 3.b)

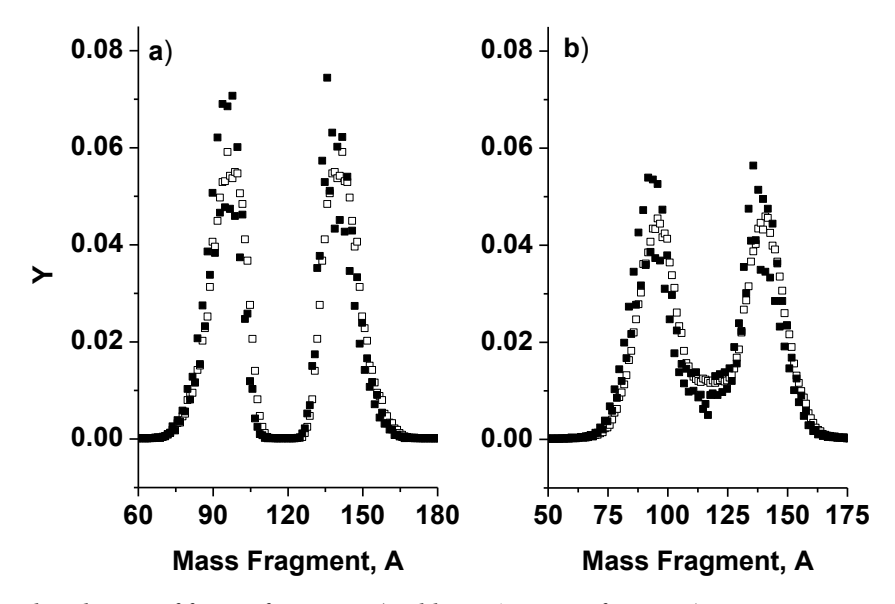


Figure 2. Mass distribution of fission fragments (Yields, Y, A = mass fragment). Neutron energy,  $E_n$ . a)  $E_n = 1$  MeV; b)  $E_n = 20$  MeV. Neutron emission: Empty squares – Pre; Black squares - Post

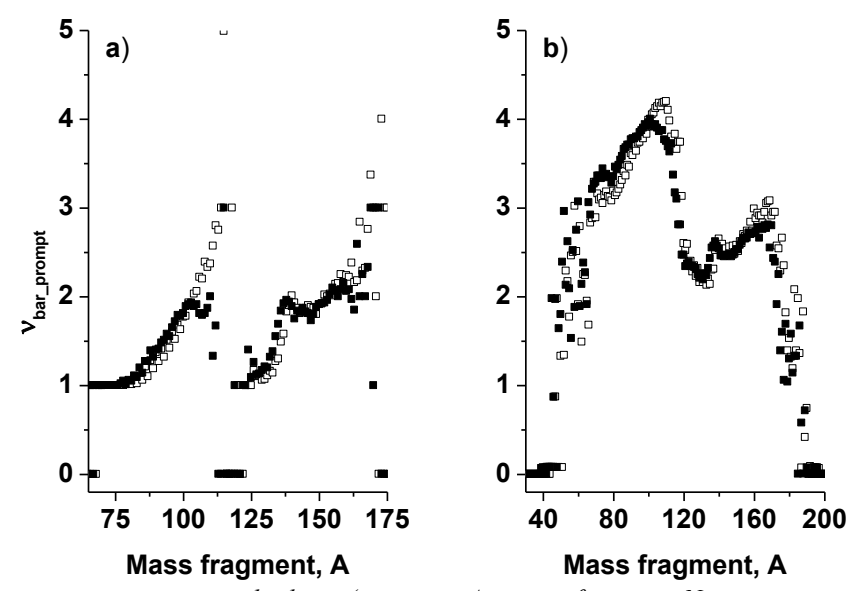


Figure 3. Average prompt neutron multiplicity ( $v_{bar\_prompt}$ . A = mass fragment. Neutron energy,  $E_n$ . a)  $E_n = 1$  MeV; b)  $E_n = 20$  MeV. Fragment mass neutron emission: Empty squares – Pre; Black squares – Post

Talys offers the capability to calculate fast and effective isotope production for a variety of applications (for example  $^{133}Xe$ ,  $^{131}I$ ,  $^{99}Mo$ , etc.). For nuclear reactors, the  $^{133}Xe$  nucleus is crucial because of its high neutron absorber properties.  $^{99}Mo$  is a widely used isotope in oncology, and the presence of  $^{131}I$  indicates a possible radioactive nuclear incident. Figure 4 illustrates the neutron's energy dependence on  $^{99}Mo$  production. In Figure 4.a, we plot the relative  $^{99}Mo$  yields, and in Figure 4.b we plot the corresponding production XS. In Figure 4, the results are obtained after neutron emission of the fission fragments (pre-neutron emission can be neglected). It has been demonstrated that fast neutrons induced fission of  $^{237}Np$  produces an order of magnitude more  $^{99}Mo$  than  $^{238}U$ . The next set of results is the neutron spectra for each incident energy for the  $^{237}Np(n,f)$  process. Figure 5 shows the events for incident neutrons with energy equal to I and 20 MeV, respectively. Figure 5.a shows that for incident energy,  $E_n = I$  MeV, compound processes produced neutrons up to 0.5 MeV.

Neutrons are produced by direct processes at higher energies, up to 2.5 MeV. Most of these neutrons come from other nuclear reaction mechanisms (n,n), (n,n'), and  $(n,\gamma)$ , rather than from fission.

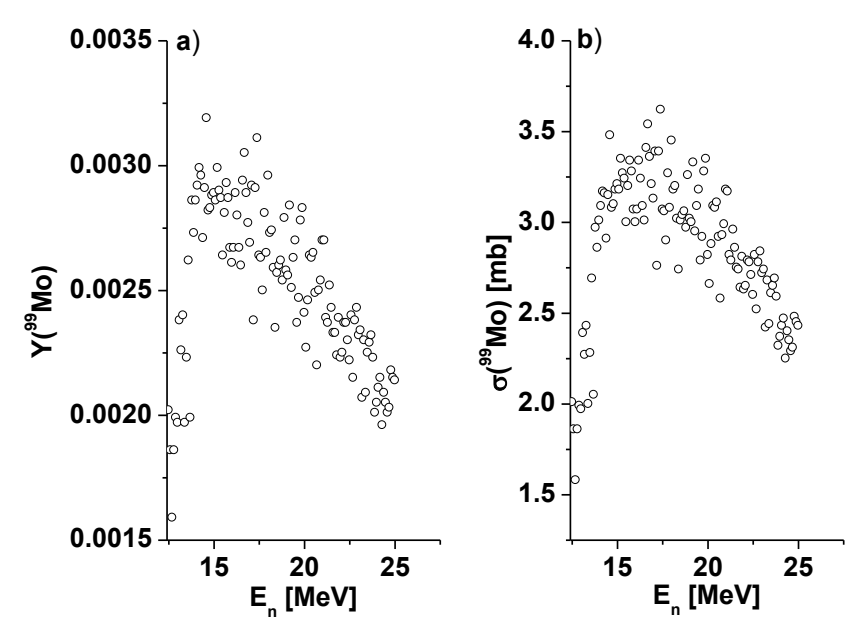


Figure. 4. The energy dependence of the production of 99 Mo isotopes. a) Yields; b) XS; Post neutron emission

As shown in Figure 5.b, for neutron incident energies up to  $\delta$  MeV the spectrum is produced by a compound process through evaporation. As compared with Figure 5.a, neutrons are produced as a result of multiemission pre-equilibrium processes in the beginning of the spectrum. Additionally, the pre-equilibrium mechanism is present throughout the entire energy range. Direct processes become dominant for neutrons with energies above 20 MeV. In all cases, preequilibrium and multipreequilibrium mechanisms contribute mainly at low energy when competing with compound processes. In order to calculate the neutron spectra shown in Figure 5.b, we accounted for all possible exit channels associated with the neutron interaction with  $^{237}Np$ . As a result of theoretical calculations, we have determined that the most important channels are fission, gamma, and neutrons. Due to the high Coulomb barrier, emerging channels such as protons, alpha particles, deuterium, and tritium can be neglected. The neutrons shown in Figure 5.b are not only caused by excited fission-induced fragments, but also by excited nuclei resulted in the inelastic, capture, and (n,xn) interactions.

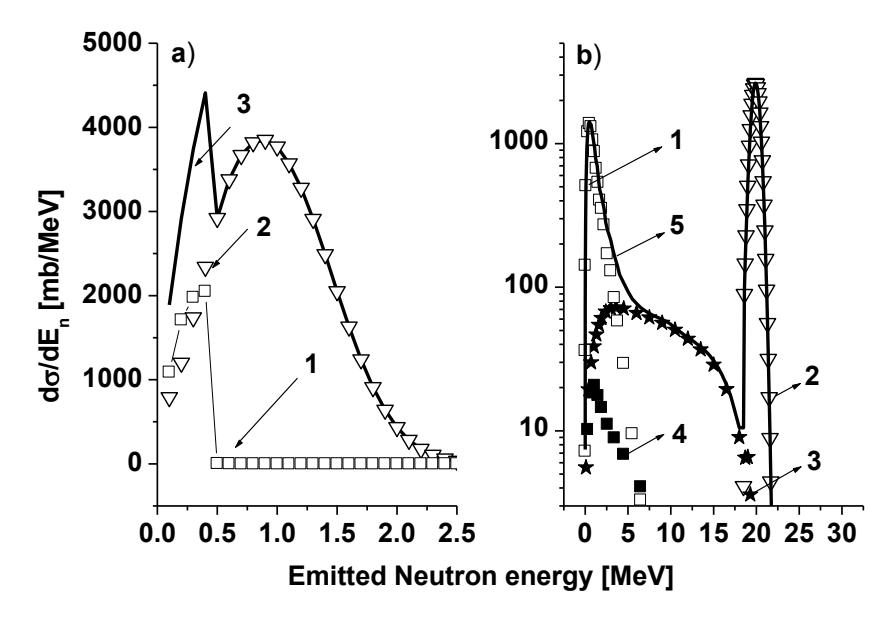


Figure 5. Reaction mechanisms contributing to neutron spectra related to incident neutron energies. a) 1 MeV; 1 – compound; 2 - . direct – 3 – total; b) 20 MeV; 1 – compound; 2 – direct, 3 – pre-equilibrium; 4 – multi pre-equilibrium; 5 - total

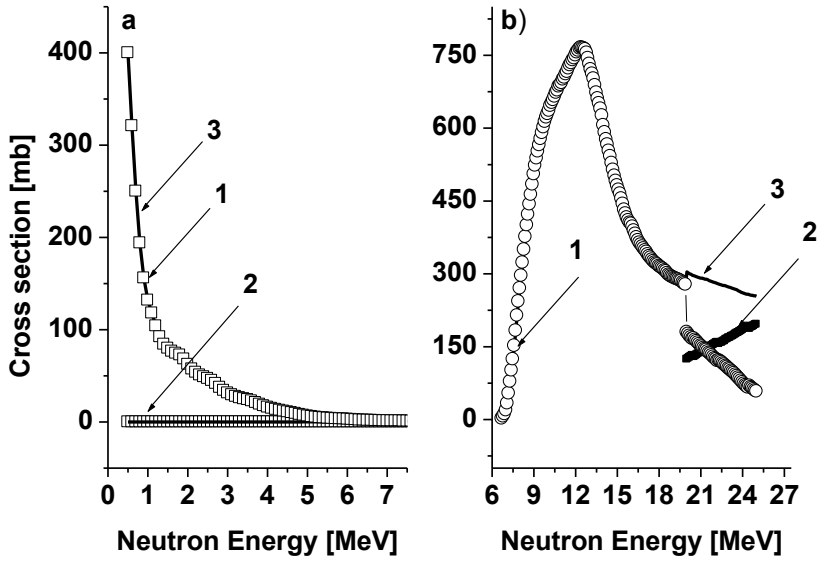


Figure 6. Np isotopes production. a) <sup>238</sup>Np; b) <sup>236</sup>Np. Processes. 1 compound; 2 – pre-equilibrium; 3 – total

As a result of the interaction of fast neutrons with  $^{237}Np$ , isotopes of Np, U, Pa, and other fissionable nuclei are produced. As well as contributing to the fission chain reaction, these nuclides are useful in the design of nuclear reactors. Compared to Np isotopes, U, Pa, and other isotopes obtained by the emission of light charged particles present lower XS production values, and their contributions to fission can be neglected. In Figures 6.a and 6.b, the production cross-sections of  $^{238}Np$  and  $^{236}Np$  are shown along with the contribution of the nuclear reaction mechanism.  $^{238}Np$  isotope is derived by the neutron capture process of  $^{237}Np$ , which can be explained essentially only by the compound mechanism. The  $^{236}Np$  nucleus is created in the  $^{237}Np(n,2n)$  reaction. Here, too, compound processes are dominant, but at higher energies, they are transformed into pre-equilibrium multistep compound processes. For both cases in Figures 6.a and 6.b, the direct mechanism has a very low value in

comparison with the compound mechanisms. A theoretical evaluation of fission variables was performed in the present study, enabling all nuclear reaction mechanisms to be investigated. For elastic and inelastic scattering, 30 levels of residual nuclei were taken into account, and for reaction channels, 10 levels. For excitation energies higher than the last discrete level, the residual nuclear states are considered in the continuum. Calculations involving the fission process were made considering a double-humped barrier. The parameters of the first barrier are: height is 6 MeV, width is 0.6 MeV, and triaxiality with left-right asymmetry type of axiality. The parameters of the second barrier are: height = 5.25 MeV; width = 0.6 MeV and left-right asymmetry as type of axiality. We used optical potentials with volume, surface, and spin-orbit components implemented in Talys for the incident and emergent channels. In the incident channel, " $n + \frac{237}{Np}$ " parameters of optical potential are: real part of volume Wood – Saxon potential, VV = 46.52 MeV, imaginary part of Wood = Saxon potential, WV = 0.08 MeV, Imaginary part of surface potential, Wd = 2.32 MeV, Real part of spin – orbit interaction, WSO = 5.69 MeV. A description of the Wood - Saxon optical potential, its notations, components, and parameters can be found in (Koning et al., 2007).

#### 4. Conclusions

Observables such as cross-sections, mass distributions, prompt neutron emissions, isotope production, and neutron spectra, which are necessary for designing an intense neutron source based on  $^{237}Np$  fuel, were analysed. For incident neutrons from 0.4 MeV to 25 MeV, calculations were carried out with the Talys software and the author's own calculations. Cross-section experimental data from literature up to 10 MeV are well described by our computed values. Based on the cross-section results, other fission observables were calculated, in the absence of experimental data. We have obtained a separation of the contributions of different nuclear reaction mechanisms in neutron spectra. As new theoretical data, over 20 fission products of interest for applications were determined in terms of yields and production cross-sections. In the fast neutron fission of  $^{237}Np$ , among all the isotopes, the  $^{99}Mo$  nucleus was chosen because theoretical evaluation had shown that it is produced ten times more than in the fast neutron fission of  $^{238}U$ .

#### References

- Aksenov, V. L., Ananev, V. D., Komyshev, G. G., Rogov, A. D., Shabalin, E. P. (2017). "On the limit of neutron fluxes in the fission-based pulsed neutron sources", *Physics of Particles and Nuclei Letters*, vol. 14, no. 5, pp. 788-797.
- Aksenov, V. L. (2017). "A 15-year forward look at neutron facilities in JINR", *JINR Dubna Preprint E3-2017-12*, pp. 1-23.
- Thomassin, A., Perrin, M. L., Gaillard-Lecanu, E., Chambrette, V., Brenot, J., (2001). *Neptunium-237, fiche radionucleide*, IPSN, première edition.
- Audi, G., Berssilon O, Blachot, J., Wapstra, A. H. (2003). "The NUBASE evaluation of nuclear and decay properties", *Nuclear Physics A*, vol. 729, pp. 3-128.
- Audi, G., Wapstra, A. H., Thibault, C. (2003), "The AME2003 atomic mass evaluation: (II). Tables, graphs and references", *Nuclear Physics A*, vol. 729, p. 337-676.
- Shabalin, E. P., Aksenov, V. L., Komyshev, G. G., Rogov, A. D. (2017). "Highly intense pulsed neutron source based on Neptunium", *Preprint JINR Dubna, P13-2017-57*, pp. 1-18.

- Shabalin, E. P., Ryazin, M. V. (2017). "Dynamics of power pulses in the Neptunium research reactor", *Preprint JINR Dubna, P-13-2017-69* pp. 1-12.
- Shabalin, E. P., Pogodaev, G. N. (1966). "On the optimization of fast neutrons impulse reactors", *JINR Dubna Communication*, no. 2708 (in Russian).
- Koning, A. J., Hilaire, S., Duijvestijn, M. C. (2007), "TALYS-1.0", Proceedings of the International Conference on Nuclear Data for Science and Technology, April 22-27, Nice, France, editors Bersillon, O., Gunsing, F., Bauge, E., Jacqmin, R., and Leray S. (2008). EDP Sciences, pp. 211-214.
- Koning, A. J., Hilaire, S., Goriely, S. (2008). "Global and local density models", *Nuclear Physics A*, vol. 810, pp. 13-76.
- Koning, A., Rochman, D. (2012). "Modern Nuclear Data Evaluation with the TALYS Code System", *Nuclear Data Sheets*, vol. 113 pp. 2841–2934.
- Koning, A., Rochman, D. (2011). "Modern nuclear data evaluation: Straight from nuclear physics to applications" *Journal of Korean Physical Society*, vol. 59, pp. 773.
- Hauser, W., Feshbach, H. (1952). "The inelastic scattering of the neutrons", *Physical Revue* vol. 87, pp. 366-373.
- Hill, D. L., Wheeler, J. A. (1953). "Nuclear constitution and the interpretation of fission phenomena", *Physical Revue*, vol. 89, pp. 1102-1145.
- Brosa, U., Grossmann, S., Muller, A. (1990). "Nuclear scission"; *Physical Reports*, vol. 197, pp. 167-262.
- Mamdouh, A., Pearson, J. M., Rayet, M., Tondeur, F. (2001). "Fission barriers on neutron-rich and superheavy nuclei calculated with ETFS method", *Nuclear Physics A*, vol. 679, pp. 337-358.
- Strutinsky, V. M. (1968). "Shells in deformed nuclei", *Nuclear Physics A*, vol. 122, pp. 1-33.
- Diakaki, M., et al., (n\_TOF Collaboration) (2016). "Neutron-induced fission cross section of <sup>237</sup>Np in the keV to MeV range at the CERN n\_TOF facility", *Physical Revue* C, vol. 93, 034614.
- Jiacoletti, R. J., Brown, W. K., Olson, H. G. (1972). "Fission Cross Sections of Neptunium-237 from 20 eV to 7 MeV Determined from a Nuclear-Explosive Experiment", *Nuclear Science and Engineering*, vol. 48, pp. 412.
- Ruskov, I., Goverdovski, A., Furman, W. I., Kopatch, Yu. N., Shcherbakov, O., Hambsch, F. J., Oberstedt S. and Oberstedt A. (2018), "Neutron induced fission of <sup>237</sup>Np status, challenges and opportunities", EPJ Web of Conferences, vol. 169, 00021.